INTENSITY OF THE AUSTRALIAN OMEGA SIGNAL OBSERVED BY THE AKEBONO SATELLITE: COMPARISON WITH A FULL WAVE CALCULATION

I. Nagano,[1] P. A. Rosen,[1] S. Yagitani,[1] K. Miyamura,[1] M. Hata,[1]
I. Kimura,[2] K. Hashimoto,[3] and T. Okada[4]

[1] Dept. of Electrical and Computer Eng., Kanazawa University, Kanazawa 920, Japan
[2] Dept. of Electrical Eng. II, Kyoto University, Kyoto 606-01, Japan
[3] Dept. of Electrical Eng., Tokyo Denki University, Tokyo 101, Japan
[4] Dept. of Electronics and Information Eng., Toyama Prefectural University, Toyama 939-03, Japan

1. Introduction

The VLF instrument on board Akebono, launched on February 21, 1989, was designed to investigate the behavior of plasma waves associated with accelerated auroral particles, wave-particle interaction mechanisms, and propagation characteristics of whistler-mode waves in the magnetosphere. The VLF instrument continues to provide high quality observations of such interesting ELF/VLF emissions as triggered emissions, ELF emissions occurring near the magnetic equator, and hiss-type emissions associated with the aurora (1). In addition to these natural noise signals, Omega navigation signals have often been observed in the magnetosphere by the VLF wide band (WB) and Poynting flux (PFX) receivers (2,3). Analysis of these coherent signals gives wave normal and Poynting flux directions, as well as the refractive index of the plasma. The signals are also very useful for calibrating the wave instruments.

Akebono observed the Omega signal for a short period on October 9, 1991 at an altitude of about 1000 km, when the spacecraft passed directly over the Australian Omega transmitting station. In this paper, the characteristics of the Omega signal obtained by the PFX receivers are studied using the analytic signal method. The observed field intensities are compared with values obtained from a full wave calculation that includes the Omega signal source on the ground.

2. Observations

Akebono is tracked by four different ground stations, covering almost all orbits. While the satellite is tracked, the acquired data are relayed in real-time to the stations in a PCM data stream. Measurements performed when the satellite is not tracked are stored by the on board 8 Mbyte Bubble Data Recorder (BDR). We tried to observe 10.2 kHz Omega signals over their transmitting stations using the BDR when the satellite was near perigee. Out of ten candidate orbits, in one, the spacecraft passed directly over the Australian Omega station (147.93°E, 38.48°S in geographic coordinates). The Australian Omega signal was measured by the PFX system during the pass from north to south for 2.5 minutes, from 01:43:30UT to 01:46:00UT on October 9, 1991, corresponding to altitudes 1305 to 994 km, respectively. The Australian 10.2 kHz Omega signal pulses last 1.2 seconds and are transmitted every 10 second, for a total of 15 pulses in the time interval studied. The PFX system (1) measures three components of the magnetic field and two of the electric field in a 50 Hz bandwidth at a selectable center frequency (in this case 10.2 kHz). The five field components are sampled with 12 bits and compressed to 8 bits. Preliminary calibration methods for these data (1) did not completely compensate for phase differences between the five PFX receivers. The analytic signal method used here allows straightforward phase calibration.

3. Characteristics of the Omega analytic signal

The digital PFX data of the Australian omega signal were studied with the analytic signal method. Previous studies of the wave vector and Poynting flux of Omega signals have interpreted the real voltage samples directly (1,2,3), with the disadvantage that the samples do not easily yield their instantaneous amplitude and phase. We have adapted coherent signal processing techniques that reduce real time samples to their complex, analytic signal representation (4) to examine the PFX observations.

The analytic signal representation of a real signal $r(t)$ is the sum

$$z(t) = r(t) + i\mathcal{H}\{r(t)\},$$

where $\mathcal{H}$ is the Hilbert transform operator and $i = \sqrt{-1}$. Whereas $r(t)$ is a real signal, $z(t)$ is intrinsically complex. The analytic signal is extremely useful for narrow band signal analysis. For signals of the form $A(t)\cos(\omega_0 t + \phi(t))$, if $A(t)$ and $\phi(t)$ are band-limited, then it is easy to show that $z(t) = A(t)e^{i\phi(t)}e^{i\omega_0 t}$, *i.e.* $|z(t)|$ is the envelope of the cosine and $\arg\{z(t)\}$ is the phase of the signal. For narrow band signals in noise such as Omega signals, this representation has the distinct advantage that each complex sample is a record of the instantaneous magnitude and phase. Furthermore, calibration of the PFX system for gains and inter-channel phase differences is straightforward for data represented as the analytic signal.

After calibration, the five components of $\vec{E}$ and $\vec{B}$ measured by the PFX system are in standard phasor form. The refractive index in the standard approximation

$$n = \frac{cB_z}{u_{k_x}E_y - u_{k_y}E_x}$$

is in general complex and is sensitive to uncompensated phase differences among the E and B channels. For a plane wave propagating in homogeneous cold plasma, we expect the refractive index to be real, *i.e.*, with zero phase.

Figure 1 shows Akebono observations of an Omega signal pulse transmitted by the Australia station. Plotted in the figure are calibrated measurements $|E_x|$ and $|B_x|$, and the inferred $|E_z|$ and complex refractive index n. Though only the field magnitudes are plotted, the phases of the measurements are available and were used to compute E_z and n. The first 0.6 seconds of the pulse are not usable because of improper gain settings in the PFX system. The receiver recovers for the remainder of the pulse, and the signal in this region is very well behaved. Note in particular that the phase of the refractive index is nearly zero in the valid region of the pulse, indicating that the inter-channel phases are properly compensated in the calibration. The refractive index can be used to determine a local electron density according to the Appleton-Hartree equation. The PFX-inferred electron density is a reference mark for the electron density profile assumed in the full wave calculation, as described below.

Figure 2 shows the Omega analytic signal intensities of B_x in a geographical coordinate system, when Akebono passed directly over the Australian station. The trajectory is marked with an arrow. The lines perpendicular to it are the signal intensities in the 15 pulses studied. The strongest intensity measured was 3.8 pT rms at a position of about 180 km northward from the source. The star in the figure indicates the position of the station. The circle shows the point at 1000 km altitude through which Earth's magnetic field line connecting to the Omega station passes.

4. Full wave calculation and discussion

We have developed a full wave method for calculating wave intensites in the ionosphere radiated from a source located at some height above sea level (5). We have applied this method to calculate the Omega intensities at the satellite's altitude level above the transmitter. Figure 3 shows a map of the magnetic component of the Omega signal intensity at an altitude of 1000 km calculated by this method, assuming that the ionosphere is a horizontally stratified medium, and the transmitter antenna is a vertical dipole

located at some altitude above a plane conducting medium at sea level. The assumed transmitter power is 10 kW (6). This calculation includes waves reflected from Earth's surface. The electron density was the IRI model matched at 1000 km altitude to an electron density inferred from the observed refractive index described above. The 0 dB level corresponds to 1 pT. The thick line in the figure follows the Akebono trajectory. The origin of the coordinates (0E,0N) corresponds to the source point. The main asymmetry exists about the east-west line, because the wave propagates toward the north along Earth's magnetic field line, as expected. The distribution is asymmetrical about the north-south line as well. This is a result of a wave guiding effect along the ground, which in the southern hemisphere skews the field to the east (7). The dip of the field intensity in the center of the highest intensity region is due to the vertical dipole-like radiation pattern of the Omega transmitting antenna.

Figure 4 compares the Omega signal wave intensities observed by Akebono to the calculated values along the trajectory line plotted in Fig. 3. The 0 dB level in Fig. 4 is set at 1 pT rms. Each point along the dotted line is the average value of the observed B_x field intensity in an Omega pulse. The error bars mark the maximum and minimum values in the pulse. The solid line is the calculated profile. The shapes of the calculated and observed intensities as a function of time are quite similar. In particular, the bump at 60 seconds past the time origin of the plot is reproduced in both profiles, and the absolute maxima of both profiles nearly align. However, the calculated values are higher than those observed by 8 to 2 dB for all points measured across the pass. This is a preliminary calculation, for which the geometries of the calculation and the observations were only approximately aligned. Furthermore, some of the discrepancy may be due to differential absorption across the pass of the wave penetrating the D region, or an incorrect assumption about the radiation characteristics of the Omega antenna. The exact reasons are currently being studied; given these unmodelled uncertainties, the agreement is fairly good.

The observed intensities at the beginning and end of the plot in Fig. 4 have large fluctuations within each Omega pulse, and from pulse to pulse. The wave vector $\vec{k}$ and Poynting vector $\vec{P}$ do not converge to single values in these disturbed regions, while the $\vec{k}$ direction converges nicely to a direction about 20° from Earth's magnetic field line and $\vec{P}$ is almost parallel to the field line in the unperturbed region. The perturbed region is well above the expected system noise level, so we are observing physical fluctuations of the signal in the plasma. At the moment, we have no explanation for this behavior.

Acknowledgments

The authors thank Prof. K. Tsuruda, Akebono project manager, and the Akebono tracking team. Part of this work was supported by the Betsukawa Foundation.

References

(1) I. Kimura *et al.*, *J. Geomag. Geoelectr.* **42,** 459-478, 1990.
(2) A. Sawada *et al.*, GRL, **18,** 321-324, 1991.
(3) M. Yamamoto *et al.*, GRL, **18,** 325-328, 1991.
(4) A. Oppenheim and R. Shafer, *Digital Signal Processing*, Prentice Hall, 1975.
(5) I. Nagano *et al.*, IEICE (in Japanese), **J74-B-II,** 285-293, 1991.
(6) E. Swanson and C.P. Kugel, Proc. IEEE, **60,** 540-551, 1972.
(7) J. Galejs, *Terrestrial Propagation of Long Electromagnetic Waves*, Pergamon Press, 1972.

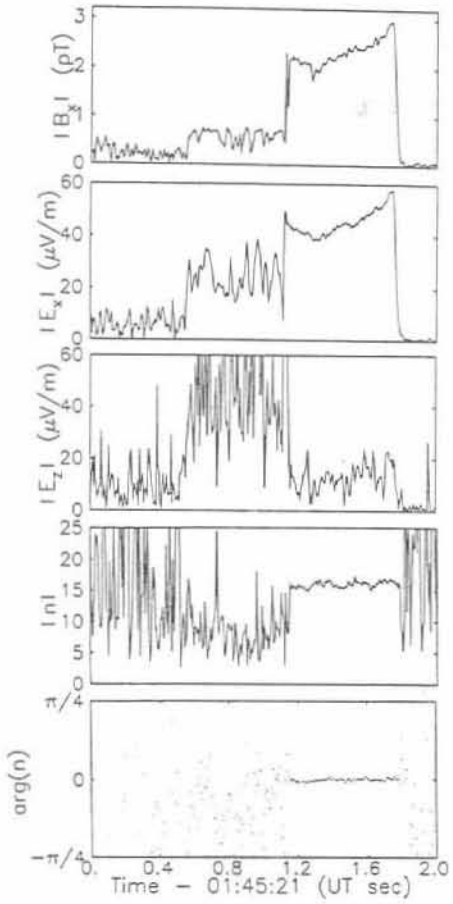

Figure 1. An example of the field components B_x, E_x, and inferred E_z of an Australian Omega pulse, and the complex refractive index inferred by the analytic signal method.

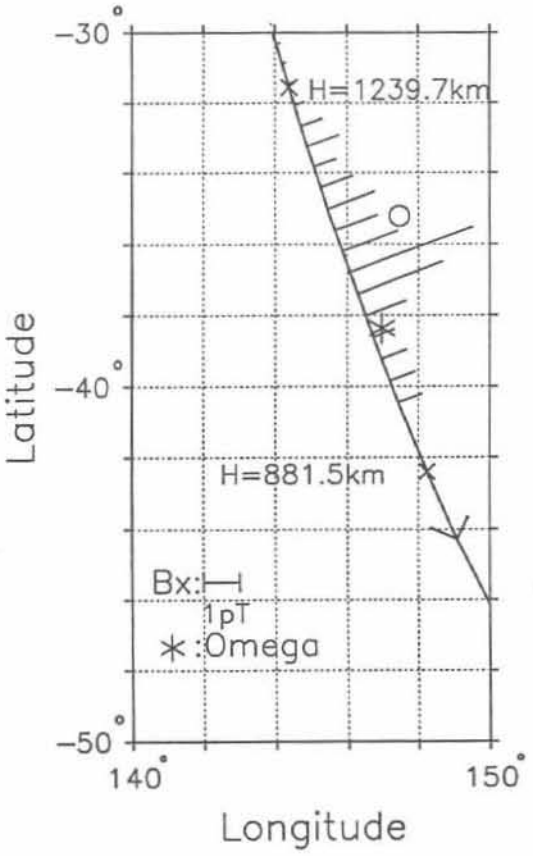

Figure 2. Omega signal intensities observed by the Akebono satellite on October 9, 1991.

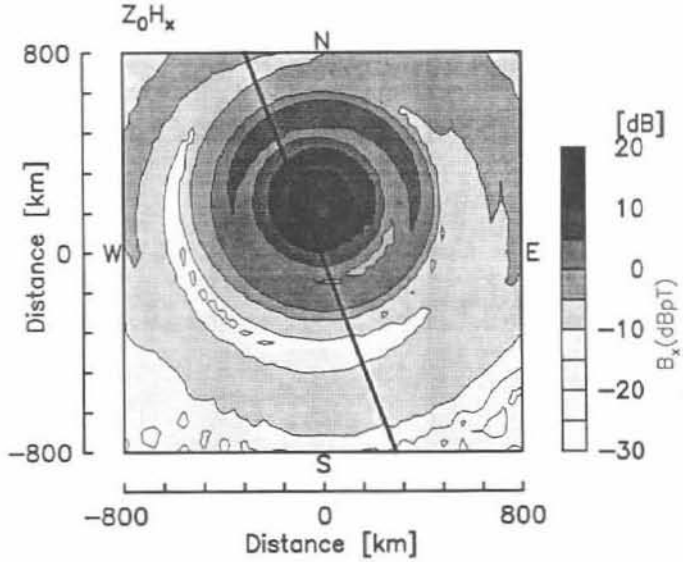

Figure 3. Map of the Omega intensites calculated by a full wave method.

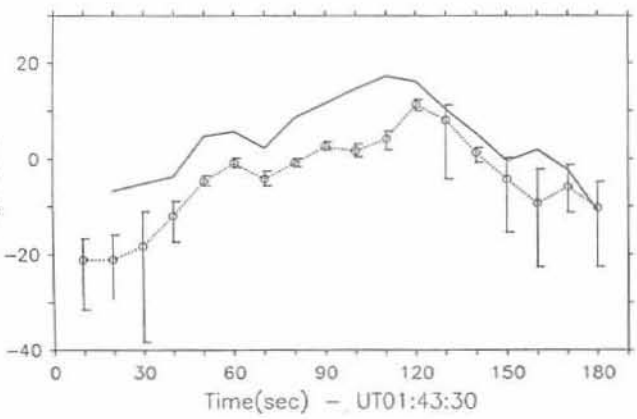

Figure 4. Comparison of the calculated full wave field intensities with those observed along the Akebono trajectory.